Nucleation times in the two-dimensional Ising model

Kevin Brendel, G. T. Barkema, and Henk van Beijeren
Theoretical Physics, Utrecht University, Leuvenlaan 4, 3584 CE Utrecht, the Netherlands
(Received 20 August 2003; published 11 March 2005)

We consider the distribution of nucleation times in systems with Brownian type dynamics, as described by classical nucleation theory. This is studied for a prototype system: the two-dimensional Ising model with spin-flip dynamics in an external magnetic field. Direct simulation results for the nucleation times, spanning more than four orders of magnitude, are compared with theoretical predictions. In contrast to usual treatments we determine size-dependent droplet free energies and effective transition rates for growth and shrinkage directly from our simulations. The free energies so determined are well described by the classical Becker-Döring expression, provided one uses an effective surface tension that exceeds the macroscopic surface tension by up to 20%. Within this framework there is good agreement between simulation results and theoretical predictions for the mean nucleation time. In addition we consider the short-time behavior of the nucleation probability after an initial quench into the metastable state. We present theoretical estimates and show that these too agree well with simulation results.

DOI: 10.1103/PhysRevE.71.031601 PACS number(s): 64.60.Qb

I. INTRODUCTION

Homogeneous nucleation is a prototypic example of escape from a metastable state through thermal activation. In this process a stable nucleus spontaneously grows in a metastable environment. It has been studied extensively, and excellent books and reviews exist [1,2]. A commonly used system for studying nucleation phenomena is the well-known Ising model. Above the so-called critical temperature, in the absence of an external magnetic field, up-and down-pointing spins are roughly equally abundant. Below the critical temperature, the system prefers to be in either of two states: one state with a positive magnetization, in which most spins are pointing up, and the other state with a negative magnetization. In the presence of an external field one of these states is metastable and will decay to the stable equilibrium state through nucleation.

The dynamical and statistical characteristics of this process are the subject of *classical nucleation theory* (CNT), which was founded in the first part of the last century by Volmer and Weber [3], Farkas [4], Becker and Döring [5] and Zeldovich [6], among others. In this theory the process is described as the stochastic growth of a droplet, which may grow or shrink by the attachment or detachment of single molecules. The rates for these elementary processes are assumed to satisfy a detailed balance condition determined by the free energy of the droplet. In its simplest form this free energy consists of the following two contributions: a bulk contribution equal to the number of particles in the cluster times the chemical potential difference between the stable and the metastable state (also called the supersaturation), and a surface contribution equal to the surface area times the surface tension, which is supposed to be the same as that for coexisting states in equilibrium. The shape of the droplet is assumed to be isotropic (circular in two, spherical in three dimensions). For small droplets the surface term dominates and the droplet free energy increases with size. For large droplets the bulk term dominates. The free energy as a function of cluster size C, expressed in the number of molecules within the cluster, will therefore have a maximum at a critical cluster size C_x. For small supersaturation, the chemical potential difference $\Delta F \equiv F(C_x) - F(0)$ is typically large compared to $k_B T$, with T temperature and k_B Boltzmann's constant. Nucleation is thus a thermally activated process and the *nucleation rate*, i.e., the average number of nucleations per units of volume and time is suppressed by an Arrhenius factor $\exp[-\Delta F/(k_B T)]$.

Homogeneous nucleation rates are not easy to measure experimentally, but in the literature there are many reports of simulation work in which homogeneous nucleation rates have been computed. Several authors claim good agreement with classical nucleation theory [7–9], but many authors mention the need for corrections to the CNT expression for the cluster free energy. Notably, Auer and Frenkel [10] numerically found that the surface tension of a fairly small cluster of solid immersed in the liquid phase of a hard sphere system under metastable conditions, is markably beyond the macroscopic surface tension of an equilibrium solid-liquid interface at the same temperature. The same had been observed in real experiments on nucleation in colloidal suspensions [11] and similar results were obtained by density functional and similar calculations [12]. For the two-dimensional Ising model Acharrya and Stauffer [13] claim rough agreement with CNT, but require a surface tension that is roughly $4/3$ times the macroscopic value. Shneidman, Jackson, and Beatty [14] use exact results to estimate the free energy for very small clusters, but for larger ones they use the expression from CNT with a constant shift based on the exact small cluster free energies. Neuhaus and Hager [15] list several finite-size and curvature corrections to the surface tension, but do not evaluate their quantitative importance under specific conditions.

Here we first of all show that for the two-dimensional Ising model under nonconserving dynamics CNT, and specifically the Becker-Döring equations, work very well, provided one uses realistic values for the cluster free energies combined with effective transition rates that are based on

global properties of the interface dynamics and that exhibit a proper dependence on cluster size. Under these conditions we find nucleation rates that differ never more than 20% from their theoretical values, although the range of values found spans over four decades.

In addition we calculate the effects of an initial quench from a high temperature or positive field state into the metastable state. Right after the quench only very small droplets of the stable phase may be found. This first of all gives rise to an asymptotic time shift in the nucleation time distribution, which can be calculated in terms of the parameters of the Becker-Döring equations. This time shift is independent of system size and therefore becomes relatively more important as the system gets larger. Secondly, from the Becker-Döring equations we also obtain the short-time probability distribution function for nucleation after an initial quench, which differs from the Poisson distribution that holds asymptotically for large times (but still small enough that the clusters that have nucleated already, cover only a negligible fraction of the total surface area). Both the asymptotic time shift and the short-time nucleation probability thus obtained show very good agreement to simulation results.

The organization of our manuscript is as follows. In Sec. II, we describe the Ising model with spin-flip dynamics, the model that we study in detail. Next, in Sec. III, we outline the theoretical framework and apply it to our model. In Sec. IV we compare the theoretical predictions with the results of high-accuracy computations, and in the final section we discuss our results.

II. DETAILED DESCRIPTION OF THE MODEL

We consider the Ising model on a square lattice with lateral dimension L, periodic (helical) boundary conditions, and an external magnetic field h which favors downward-pointing spins. The Hamiltonian of this model reads

$$H = -J\sum_{\langle i,j\rangle} s_i s_j + h\sum_i s_i, \tag{1}$$

in which $s_i = \pm 1$ is the spin at site i, and J is the coupling constant. The first summation runs over all pairs of nearest-neighbor sites; under our helical boundary conditions the neighbors of site i are $j = i \pm 1$ modulo N and $j = i \pm L$ modulo N, with $N = L^2$. Note that in the sum each pair is counted only once. The magnetization is defined as $M \equiv \Sigma_i s_i$; it can take values $M = -N, -N+2, \ldots, N$. We restrict ourselves to systems in which L is even. As a consequence, M takes only even values, and summations over a range of possible magnetizations only run over even numbers, with an increment of 2.

The system evolves in time according to single-spin-flip dynamics with Metropolis acceptance probabilities [16]. If S_i is the configuration after i proposed spin flips, a trial configuration S'_{i+1} is generated by flipping a single spin at a random site. This trial configuration is then either accepted ($S_{i+1} = S'_{i+1}$) or rejected ($S_{i+1} = S_i$); the acceptance probability is given by

$$P_a = \min[1, \exp(-\beta\{E(S'_{i+1}) - E(S_i)\})], \tag{2}$$

in which $\beta = 1/(k_B T)$ with k_B Boltzmann's constant and T temperature. Our unit of time is one Monte Carlo step per site (MCSS), so in one unit of time N Monte Carlo steps are performed and *on average* each spin is proposed to be flipped once.

In a previous publication [17] we applied the same method to estimate the distribution of magnetization reversal times in an Ising model on a finite lattice in the absence of a magnetic field. This is a very similar activated process: the intermediate state of high free energy in this case consists in a state with a strip of opposite magnetization separated from the original bulk state by two straight interfaces. Theoretically this system is somewhat easier to treat, because more is known about straight interfaces in the absence of a field than about the interface between a droplet and the bulk.

III. THEORETICAL FRAMEWORK

To study the behavior of nucleation times at temperatures below the critical one we consider an ensemble of systems prepared in configurations with no large negative clusters present (typically by quenching from a positive field equilibrium state). For each system in the ensemble we keep track of the sizes of all of its clusters. These are geometrical clusters, defined as sets of aligned spins, interconnected by bonds between nearest-neighbor sites and completely surrounded by spins of opposite sign. They are equivalent to Coniglio-Klein clusters [18] in the limit of zero temperature, and do not differ much from these at the temperatures considered here. The sizes of our clusters are defined as the numbers of aligned spins contained in them. We define the nucleation time of a system as the first time at which one of its clusters grows beyond a given size A, which is comparable to but larger than the critical cluster size for reasons that will be made clear below. For a theoretical description we would like to derive an expression for the probability distribution of the nucleation time under the stochastic dynamics of the system.

The spin-flip dynamics described in Sec. II may be represented by a master equation for the probability distribution $P(\mathbf{S}, t)$ of finding a system in the configuration $\mathbf{S}$ at time t. Due to the huge number of possible configurations this master equation cannot be solved analytically or even numerically for system sizes of practical interest. Therefore we resort to a couple of approximations that are made standardly in classical nucleation theory. First, we assume that we may treat the clusters of negative spins in the system as being independent. In this approximation, the probability that none of the N_c clusters has grown beyond the critical size, is simply the N_c^{th} power of the probability that a single cluster has not grown beyond the critical size. Secondly, following the Becker-Döring approach [5], we assume that the dynamics of a single cluster may be modeled by a master equation for the probability $P(C, t)$ that this cluster contains C spins at time t:

$$\frac{dP(C,t)}{dt} = \Gamma_{C,C+1}P(C+1,t) + \Gamma_{C,C-1}P(C-1,t) - (\Gamma_{C+1,C} + \Gamma_{C-1,C})P(C,t). \tag{3}$$

By adopting this equation we make several approximations:

we suppress all dependence of the transition rates on the shape of the clusters and we neglect the possibilities of merging or splitting of clusters. In Sec. IV B and V we will come back to this and argue how these effects can be accounted for to a large extent by choosing the transition rates in Eq. (3) in an appropriate effective way.

In order that the equilibrium distribution of cluster sizes be a stationary solution of the master equation we impose the condition of detailed balance

$$\frac{\Gamma_{C+1,C}}{\Gamma_{C,C+1}} = \exp\{\beta[F(C) - F(C+1)]\}, \tag{4}$$

where $\beta F(C) = -\ln[P_{eq}(C)/N]$, with $P_{eq}(C)$ the average number of clusters of size C for a system forced to be in equilibrium in the metastable state (see Sec. IV A). For C large enough that it is very improbable to find more than one cluster of size C simultaneously in the metastable system, $P_{eq}(C)$ may likewise be interpreted as the probability of finding a cluster of size C in it.

The long-time nucleation rate as predicted by the master equation (3) follows as the largest eigenvalue (with a minus sign) of this equation, supplemented with an absorbing boundary at $C=A$. Here A is an integer larger than the critical cluster size C_x, chosen such that $P_{eq}(A) \gg P_{eq}(C_x)$, and clusters with size A are almost certain to nucleate. The absorbing boundary condition is implemented by setting $\Gamma_{A-1,A}$ equal to zero.

The largest eigenvalue $-\nu$ of $\Gamma_{C,C'}$ in Eq. (3), as well as the corresponding eigenvector $P_0(C)$, may be found by requiring that the net current away from cluster size C assumes the value $\nu P_0(C)$. Using conservation of probability one easily shows that this may be expressed as

$$j_{C+1,C} \equiv \Gamma_{C+1,C}P_0(C) - \Gamma_{C,C+1}P_0(C+1) = \nu \sum_{c \leqslant C} P_0(c), \tag{5}$$

$$\nu = \frac{\Gamma_{A,A-1}P_0(A-1)}{\sum_{c \leqslant A-1} P_0(c)}, \tag{6}$$

where $j_{C+1,C}$ is defined as the net current flowing from C to $C+1$. This current may be approximated by

$$j_{C+1,C} = \begin{cases} \nu \dfrac{\sum_{c=1}^{C} \exp[-\beta F(c)]}{\sum_{c=1}^{C_x} \exp[-\beta F(c)]}, & c \leqslant C_x, \\ \nu, & c \geqslant C_x, \end{cases} \tag{7}$$

because the sum on the right-hand side of Eq. (5) is dominated by the terms with small c-values, for which $P_0(c)$ is approximately proportional to $\exp[-\beta F(c)]$. This may be checked in hindsight against the solution obtained. With this approximation the equation may be solved recursively for $P_0(c)$ in terms of $P_0(A-1)$ for $c=A-2, A-3, \ldots$, with the result

$$\frac{P_0(c)}{P_0(A-1)} = \frac{\Gamma_{A,A-1}}{\nu} \sum_{m=c}^{A-1} j_{m+1,m} \frac{\exp\{\beta[F(m) - F(c)]\}}{\Gamma_{m+1,m}}. \tag{8}$$

Since the sum over m is dominated by values close to or larger than the critical cluster size, for which $j_{m+1,m}$ is approximately equal to ν, we may replace Eq. (8) by

$$\frac{P_0(c)}{P_0(A-1)} = \Gamma_{A,A-1} \sum_{m=c}^{A-1} \frac{\exp\{\beta[F(m) - F(c)]\}}{\Gamma_{m+1,m}}. \tag{9}$$

Now substituting this into Eq. (6) we arrive at the result

$$\nu = \left(\sum_{m=1}^{A-1} \frac{\exp[\beta F(m)]}{\Gamma_{m+1,m}} \sum_{c=1}^{C_x} \exp[-\beta F(c)] \right)^{-1}, \tag{10}$$

where we have used the fact that the sum over c is dominated by small values of c to extend the sum over m to $m=1$. The result in Eq. (10) is well known. It is usually derived by considering a state with a stationary current in which mass is inserted at a constant rate on one side (e.g., at $C=0$ in our case) and taken out as soon as it reaches the absorbing boundary (see, e.g., Ref. [19], Sec. IV E). In that case the replacement of $j_{m+1,m}$ by a constant is exact.

For arbitrary initial distributions $P(C,0)$ that are concentrated near the origin, one may give an even more accurate representation of the long-time behavior of $P(C,t)$, by writing it in the form

$$P(C,t) = kP_0(C)\exp[-\nu t] \quad \text{for } t \to \infty, \tag{11}$$

where k is a constant which represents the component of $P(C,0)$ along $P_0(C)$ if $P(C,0)$ is decomposed in terms of the eigenfunctions of the master equation. This gives for the probability $S(t)$ that the system has not yet nucleated at time t

$$S(t) = \sum_{C=1}^{A-1} P(C,t) = \exp[-\nu(t - t_d)] \quad \text{for } t \to \infty, \tag{12}$$

where t_d is called the delay time. The eigenfunction $P_0(C)$ was given (with a different normalization) in Eq. (8):

$$\psi^r(n) \equiv \frac{\nu}{P_0(A-1)\Gamma_{A,A-1}} P_0(n) = \sum_{m=n}^{A-1} j_{m+1,m} \frac{\exp\{\beta[F(m) - F(n)]\}}{\Gamma_{m+1,m}}, \tag{13}$$

with $j_{m+1,m}$ given in Eq. (7). As a consequence of the condition of detailed balance, Eq. (4), the corresponding left eigenvector is obtained by multiplying $\psi^r(n)$ by $\exp[\beta F(n)]$, or

$$\tilde{\psi}^l(n) = \sum_{m=n}^{A-1} j_{m+1,m} \frac{\exp[\beta F(m)]}{\Gamma_{m+1,m}}. \tag{14}$$

Notice that for small values of n this is virtually independent of n, because only the largest m values give important contributions to the sum. Using the proper normalization of the leading eigenfunction, and approximating $P(C,0)$ by $\delta_{C,1}$, one now finds immediately that t_d follows from

$$\exp[\nu t_d] = \frac{\tilde{\psi}^l(1)\sum_{n=1}^{A-1}\{\exp[-\beta F(n)]\tilde{\psi}^l(n)\}}{\sum_{n=1}^{A-1}\{\exp[-\beta F(n)][\tilde{\psi}^l(n)]^2\}}. \quad (15)$$

Now, by subtracting unity on both sides, dividing by ν, approximating sums over m from n to $A-1$ by sums from 1 to $A-1$, where appropriate, substituting Eq. (14) and using Eq. (7) for $j_{m+1,m}$, one obtains

$$t_d = \frac{\sum_{n=1}^{A-1}\sum_{m=1}^{n-1}\left(\frac{W(n)}{\Gamma_{m+1,m}W(m)}\sum_{k=1}^{\min[m,C_x]}W(k)\right)\tilde{\psi}^l(n)}{\sum_{n=1}^{A-1}[W(n)\tilde{\psi}^l(n)]}, \quad (16)$$

with $W(n) \equiv \exp[-\beta F(n)]$.

IV. SIMULATIONS AND RESULTS

For applying the above theoretical framework to nucleation times in the Ising model, the two ingredients required are (i) the cluster free energies $F(C)$ and (ii) the transition rates $\Gamma_{C',C}$ from cluster sizes C to C'. We obtain these two ingredients via two different computational tools.

In all our simulations, we use a technique known as multispin coding [20], which enables us to reach long simulation times and thus good statistics. All random numbers are generated with a lagged Fibonacci generator, as provided in Ref. [20].

A. Cluster free energies

We measure the distribution of cluster sizes for various values of β and h, in a system with 64×64 spins. We are actually only interested in the distribution of clusters smaller than a certain size A, which was discussed in Sec. III. Therefore we define a cutoff cluster size C_{max}, which is typically chosen to be 300. We modify our algorithm in the following way: starting with a configuration S_i we perform a fixed number M of Monte Carlo steps, and measure the sizes of all the clusters of down-spins in the system. If there is a cluster with more than C_{max} spins we reject the new configuration and choose $S_{i+1}=S_i$. Otherwise we accept the new configuration as our S_{i+1}. In all cases we add the sizes of the clusters in S_{i+1} to a histogram. After many repetitions of this loop we find the free energy $F(C)$ from

$$\beta F(C) = -\ln\frac{\langle N(C)\rangle}{N}, \quad (17)$$

where $\langle N(C)\rangle$ is the average number of clusters of size C in the system with N sites.

If C_{max} is chosen too large, the various clusters in the system influence each other. In particular, excluded volume effects inside and around large clusters suppress larger clusters in the metastable state more than smaller ones. As a consequence the distribution of cluster sizes depends on C_{max}. To determine whether a certain value of C_{max} is allowed, we check that the free energy curve coincides with the same curve, obtained with a lower value for C_{max}.

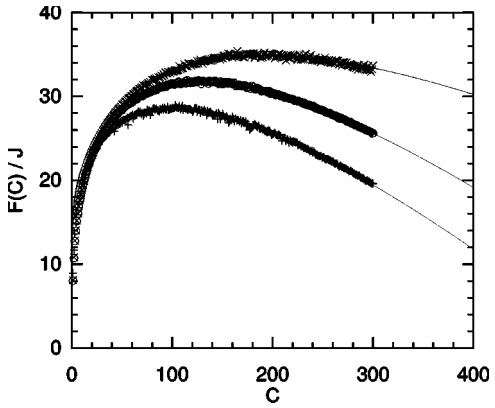

FIG. 1. Free energy as a function of cluster size in the 64×64 system at $\beta J=0.56$ and $h=0.06(\times)$, $\beta J=0.58$ and $h=0.08(\bigcirc)$, and $\beta J=0.53$ and $h=0.08(+)$. The lines represent the Becker-Döring expression, Eq. (18), with fitted values $\sigma=0.93$, 1.00, and 0.88, and $F_0=12.3$, 11.9, and 13.4.

Figure 1 shows our measurements for the free energy according to Eq. (17) as a function of cluster size, for some combinations of temperature and external field.

For large clusters, one may expect that classical nucleation theory can be used. At not too low temperatures the clusters on average are nearly circular in shape. The free energy is then approximated by the Becker-Döring expression [5]

$$F(C) \approx F_0 + 2\sigma\sqrt{\pi C} - 2hC, \quad (18)$$

where σ is the excess free energy of the interface per unit length, and h the strength of the external field.

Strictly speaking, in order to account correctly for the difference between the free energies of the metastable and the stable phase, one should replace $2hC$ by $2hC(2m_s-1)$, with m_s the average spin per lattice site. At the temperatures considered here, however, m_s is very close to unity, so this correction is very small. In two dimensions there are also physical contributions to this term, resulting from the Gibbs-Thompson effect (compression of the cluster under the influence of surface tension) and from Tolman, or curvature corrections [21]. We fitted F_0 and σ to the data in Fig. 1, and added the corresponding curves as lines in the same figure. The measurements are well fitted by the curves, as long as the cluster size is not too small. However as noted before by Shneidman *et al.* [14], the surface tensions obtained in this way are larger than those given by the Onsager expression [22]

$$\sigma = 2J + \beta^{-1}\ln\tanh(\beta J), \quad (19)$$

valid for long horizontal or vertical interfaces, and zero external field (see Fig. 2). At the temperatures we considered the surface tension is known to be almost isotropic [23], so anisotropy effects cannot explain this difference. As suggested by Fig. 2 both field dependence of the surface tension and corrections due to the finite size of the clusters play a role here. Note that similar corrections for the surface tension

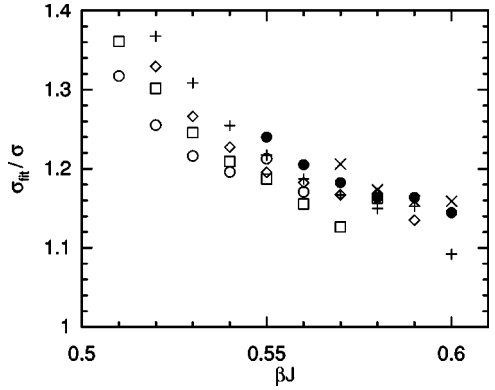

FIG. 2. Ratio of the surface tension obtained by fitting the free energy curve and the theoretical value given in Eq. (19), as a function of βJ. Different symbols denote different strengths of the external field: $h=0.05$(○), $h=0.06$(□), $h=0.07$(◇), $h=0.08$(+), $h=0.09$(●), and $h=0.10$(×).

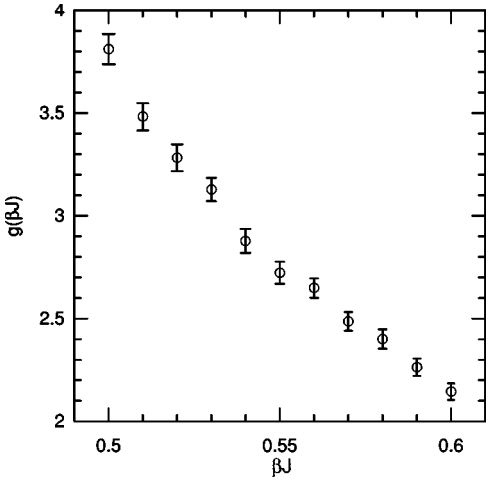

FIG. 3. Monte Carlo measurements of the diffusion coefficient per interface length $g(\beta J)$, as a function of inverse temperature βJ.

on a finite cylinder are present already in Onsager's exact solution [22]. In Ref. [17] an explicit plot of this was given. For a precise determination of nucleation rates these corrections are quite important. They may easily cause a change by a few orders of magnitude in the values of average nucleation rates. We will address these issues in more detail in a separate paper [24].

B. Interface diffusion coefficient

The second ingredient required in the theoretical framework of Sec. III is the rate $\Gamma_{C+1,C}$ of cluster growth. To estimate this rate we study the diffusion of a single interface in a system with anti-periodic boundary conditions in the absence of an external field, as described in [17]. The location of the interface is obtained from the magnetization M. The diffusion coefficient D is defined as

$$D = \lim_{t\to\infty}\left[\frac{\langle [M(t)-M(0)]^2\rangle}{2t}\right]. \tag{20}$$

This diffusion coefficient is found, to a good approximation, to depend linearly on the length of the interface B:

$$D(B,L,\beta J) = g(\beta J)B + c, \tag{21}$$

where the constant c was added to allow for potential finite-size effects. In an appendix we show that such corrections are to be expected indeed, on the basis of a simple model calculation for a two-dimensional BCSOS model. One might expect small corrections to Eq. (21) due to the helical boundary condition. However, as mentioned already, at the temperatures studied the surface tension is almost perfectly isotropic. Therefore the chief effect of the helical boundary conditions is an extension of the interface length to $\sqrt{B^2+1}$. The effect of this is exactly compensated by the fact that the relevant motion of the interface is not orthogonal to its average orientation, but under a small angle with it. The results for $g(\beta,J)$ for various temperatures are plotted in Fig. 3.

To arrive at an estimate for the rate $\Gamma_{C+1,C}$ for cluster growth and shrinkage, we assume that the diffusion coefficient neither depends on the external field nor on the shape of the interface (straight or circular), but only on the length of the cluster boundary, for which we use $2\sqrt{\pi C}$, assuming that the shape of the cluster is almost circular.

This approximation neglects the possibility of having a few positive spins inside the clusters, but at the temperatures studied this will at most amount to a systematic underestimate of the boundary length by a few percent. For large clusters the assumption of circular shape should be very good. From Eqs. (10) and (16) we see that the contributions from small clusters to the expressions for ν and t_d are almost negligible, and inaccuracy of the estimates of their boundary lengths is not very important. This then gives rise to a jump rate

$$\Gamma_{C+1,C} = \frac{g(\beta J)}{4} 2\sqrt{\pi C}. \tag{22}$$

The factor 4 arises because the jumps in magnetization go by units of 2. Alternatively, instead of $\Gamma_{C+1,C}$ we could have identified $\Gamma_{C,C+1}$ through D. The detailed balance condition (4) causes these quantities to be slightly different. However, for C-values close to the free energy maximum, which are weighted most strongly, their difference becomes very small. In addition there will be some compensating effects, because for $C \geqslant C_x$ one has $\Gamma_{C+1,C} > \Gamma_{C,C+1}$ whereas for $C < C_x$ this is just the other way around.

C. Nucleation rates

To measure nucleation rates, we first bring the system into equilibrium in the presence of a magnetic field. At time $t=0$, we then reverse all the spins (equivalent to an instantaneous reversal of the magnetic field) so that the system is near its metastable equilibrium. We measure the time the system needs to reach the magnetization corresponding to the stable equilibrium.

Nucleation has taken place as soon as a cluster has grown well beyond the critical nucleus size. Once that happens, the relatively small systems in our simulations will quickly

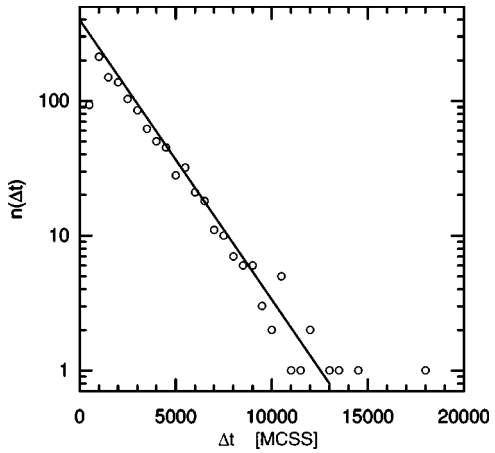

FIG. 4. Histogram of the time Δt elapsed before nucleation occurs, at inverse temperature $\beta J=0.54$ and external field strength $h=0.08$, in a system with 64×64 sites. The straight line is a fit, given by $n(\Delta t)\sim\exp(\Delta t/1990)$.

equilibrate in the state in which most spins align with the external field. Since monitoring the size of the biggest cluster is computationally demanding, we monitor instead the total magnetization, and conclude that nucleation has taken place as soon as it has reached a value corresponding to the stable equilibrium.

We make a histogram of all the measured times.

Figure 4 shows that at long times the decay function $f(t)$ behaves as $f(t)\sim\exp(-\nu_s t)$. Here, we focus on the long-time behavior, and are specifically interested in the asymptotic nucleation rate ν_s. We obtain this quantity via a fitting procedure, in which we ignore the data up to a time t_0, chosen such that $f(t)$ shows exponential time behavior for $t>t_0$. Then we determine the time t' at which half of the remaining events have taken place. We then obtain the first nucleation time $\tau\equiv\nu_s^{-1}$ from $\tau=(t'-t_0)/\ln(2)$. Instead we could have made a linear fit of all the data points beyond t_0, but this makes no significant difference. Table I gives the measured first nucleation times τ_1. In the same table, we also report the estimated first nucleation times $\tau_2=(\langle N_c\rangle\nu)^{-1}$ with ν as obtained in Eq. (10) and $\langle N_c\rangle\equiv\Sigma_{C=1}^{A}N(C)$ the average number of clusters in the system, as determined from our simulation data. Finally we also give the ratio τ_2/τ_1. The table shows that, while the values of the first nucleation times span four decades in time, the estimated and measured first nucleation times agree mostly within 20%, and in many cases even better.

D. Short-time behavior

Besides the long-time exponential behavior of the first nucleation probability, we also studied the deviations from this behavior at short times. To do so we solved the master equation (3) for the time evolution of one cluster numerically, with the initial condition that the cluster consists of a single spin:

$$P(C,0)=\delta_{C,1}. \tag{23}$$

We then computed the cumulative probability distribution $P_{nuc}(1,t)$ that the cluster has grown beyond a certain size C_{max} during time t. The corresponding probability distribution for the nucleation of one of N_c statistically independent clusters at C_{max}, at time t, is given by

TABLE I. Measured values (τ_1) and estimated values (τ_2) for the nucleation times in the 64×64 system.

βJ	h	τ_1	τ_2	τ_2/τ_1
0.51	0.04	1.83×10^4	2.26×10^4	1.234
0.51	0.05	3.35×10^3	3.84×10^3	1.146
0.51	0.06	9.84×10^2	1.14×10^3	1.163
0.52	0.04	1.07×10^5	1.09×10^5	1.019
0.52	0.05	1.13×10^4	1.31×10^4	1.153
0.52	0.06	2.84×10^3	3.57×10^3	1.257
0.52	0.07	8.51×10^2	1.09×10^3	1.276
0.52	0.08	3.96×10^2	4.49×10^2	1.134
0.53	0.05	4.15×10^4	4.79×10^4	1.153
0.53	0.06	8.94×10^3	9.47×10^3	1.059
0.53	0.07	2.31×10^3	2.57×10^3	1.111
0.53	0.08	8.98×10^2	9.59×10^2	1.068
0.54	0.05	1.73×10^5	2.13×10^5	1.228
0.54	0.06	2.90×10^4	3.11×10^4	1.071
0.54	0.07	6.69×10^3	7.27×10^3	1.087
0.54	0.08	2.17×10^3	2.32×10^3	1.068
0.55	0.05	8.03×10^5	1.13×10^6	1.410
0.55	0.06	9.57×10^4	1.08×10^5	1.126
0.55	0.07	1.97×10^4	2.08×10^4	1.054
0.55	0.08	5.60×10^3	5.98×10^3	1.070
0.55	0.09	2.05×10^3	2.17×10^3	1.058
0.56	0.05	4.02×10^6	4.59×10^6	1.140
0.56	0.06	3.78×10^5	4.17×10^5	1.103
0.56	0.07	5.81×10^4	6.44×10^4	1.109
0.56	0.08	1.48×10^4	1.57×10^4	1.058
0.56	0.09	4.92×10^3	5.11×10^3	1.038
0.57	0.06	1.47×10^6	1.36×10^6	0.927
0.57	0.07	1.84×10^5	1.98×10^5	1.080
0.57	0.08	4.14×10^4	4.40×10^4	1.062
0.57	0.09	1.24×10^4	1.24×10^4	1.000
0.57	0.10	4.02×10^3	4.53×10^3	1.128
0.58	0.06	5.80×10^6	6.60×10^6	1.139
0.58	0.07	6.18×10^5	5.72×10^5	0.926
0.58	0.08	1.10×10^5	1.26×10^5	1.143
0.58	0.09	3.06×10^4	3.11×10^4	1.015
0.58	0.10	1.13×10^4	1.06×10^4	0.938
0.59	0.07	2.25×10^6	2.48×10^6	1.104
0.59	0.08	3.49×10^5	4.22×10^5	1.209
0.59	0.09	8.47×10^4	8.36×10^4	0.987
0.59	0.10	2.31×10^4	2.47×10^4	1.068
0.60	0.08	1.04×10^6	1.19×10^6	1.145
0.60	0.09	2.05×10^5	2.52×10^5	1.229
0.60	0.10	5.81×10^4	6.72×10^4	1.156

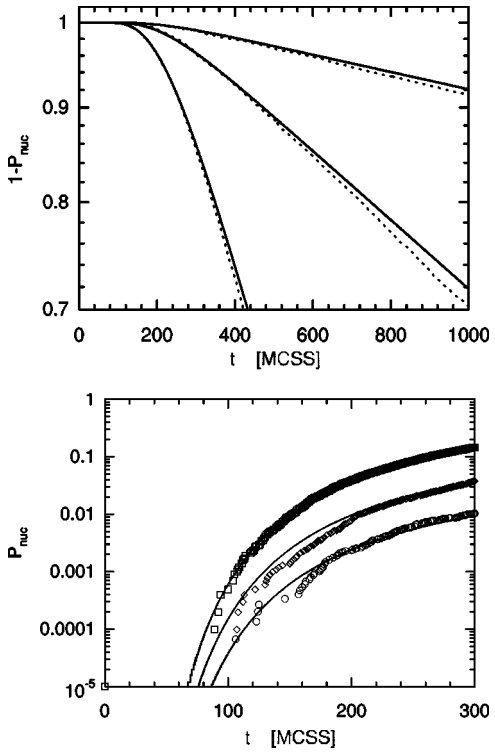

FIG. 5. $1-P_{nuc}(t)$ obtained from the time evolution of one cluster (solid lines) according to the master equation (3) combined with Eq. (24), and by direct simulation of systems with 32×32, 64×64, and 128×128 spins (the dotted lines) at $\beta J=0.54$ and $h=0.08$. In both cases, the highest of the three curves corresponds to the smallest system, and the lowest one to the largest system. The lower plot shows the same data, but focuses on short times.

$$1-P_{nuc}(N_c,t)=[1-P_{nuc}(1,t)]^{N_c}. \tag{24}$$

The quantity $P_{nuc}(N_c,t)$ should be equal to the cumulative distribution of nucleation times, if we define nucleation as the first occurrence of a cluster of C_{max} spins anywhere in the system.

We have compared this result with the results of direct simulations at $\beta J=0.54$ and $h=0.08$, for three different system sizes: 32×32, 64×64, and 128×128. In all cases the starting configuration was a system in which all spins are antiparallel to the external field. Within a few time steps this develops into a quasiequilibrium distribution for the small clusters. For the system sizes studied presently typical nucleation times are in the order of a hundred time steps, so the fact that we started from clusters of size zero rather than unity makes no real difference. Figure 5 shows the results. Here the parameter N_c was determined in the same simulations that were used to obtain the free energy as a function of cluster size.

The asymptotic slopes of the curves in the top panel of Fig. 5 correspond to the nucleation rates. The times at which straight-line fits to these curves cross $1-P_{nuc}=1$ correspond to the waiting times t_d, as introduced in Eq. (12). There is excellent agreement between the direct simulations and the parameter-free theoretical framework: The theoretical prediction obtained with Eq. (16) is $t_d=234$ MC time units, while the fits vary between $t_d=228$ and 239 MC time units. Also the behavior at short times is well described by the theoretical framework, as is evidenced in the bottom panel of Fig. 5.

For the case of the Becker-Döring form of the cluster free energy, as given in Eq. (18) the delay time has been calculated before by Shneidman *et al.* in Ref. [9], in the region where $A\gg C_x$. (These authors call it the lag time.) Under these conditions our expression (16) can be shown to reduce to

$$t_d=\frac{4k_BTC_x^{1/2}}{g(\beta J)\sqrt{\pi}}\left[\sqrt{\frac{A}{C_x}}+\ln\{2\beta h\sqrt{(A-C_x)C_x}\}+c\right], \tag{25}$$

with c a constant of order unity. For large A this fully agrees indeed with the expression of Ref. [9]. However, notice that Eq. (16) is very flexible. It holds for a wide range of forms of the free energy function and for arbitrary values of A and it can be evaluated numerically very easily.

The comparison of nucleation probabilities at late times was discussed in the preceding subsection.

V. DISCUSSION

In this paper we showed that for two-dimensional Ising models with spin-flip dynamics classical nucleation theory provides an excellent description of nucleation time distributions, provided a realistic description is used for the free energy of the growing droplets. We determined this free energy from cluster size distributions in equilibrium Monte Carlo simulations and found that it may be fitted well by the Becker-Döring expression, provided one uses surface tensions that are 10 to 20% higher than the surface tension of a bulk interface at zero field. Similar conclusions have been reached by Shneidman, Jackson, and Beatty [9], but the present paper goes into much further detail in analyzing both the cluster size dependence of the free energy and the dependence on cluster size and field strength of the effective jump rates occurring in the Becker-Döring equations. More recently Auer and Frenkel [10] studied crystal nucleation in colloidal hard sphere systems and also determined cluster free energies by monitoring the frequency of occurrence of clusters of a given size. Like us they could fit the resulting curves quite well by a Becker-Döring expression, with an effective surface tension. In their case the excess over the bulk surface tension at zero supersaturation is about 20% to 40%. They attribute the difference to a density (or chemical potential) dependence of the interfacial tension between the metastable and the stable state. In our case this corresponds to a magnetic field dependence. In Fig. 2 we see that such a dependence indeed appears to be present in our system, but quite definitely there are other corrections, due to finite cluster size, and there must also be size-independent Gibbs-Thompson and Tolman corrections. This will be discussed in more detail in a separate paper [24], together with results for three-dimensional systems.

A point one may question is whether the assumption of independent noninteracting clusters holds even for clusters of small size. This may indeed be doubted, but fortunately, at least for the asymptotic nucleation frequency $\langle \nu N_c\rangle$ this is

not really relevant. One may choose to define as clusters only those clusters that have a size $c \geqslant m_0$, with m_0 chosen such that clusters of this size already are very rare, but still $\exp[\beta F(m_0)] \ll \exp[\beta F(C_x)]$. From Eqs. (10) and (17) it then follows that

$$\nu_{m_0} = \frac{\sum_{c=1}^{C_x} N_c}{\sum_{c=m_0}^{C_x} N_c} \nu,$$

since the terms with $m < m_0$ in the first sum in Eq. (10) basically do not contribute. As a consequence of this the asymptotic nucleation rate in the system is independent of the choice of m_0.

For the short-time nucleation rate the free energy of small clusters is important indeed, especially if one starts from a state of zero magnetization. However, if one starts from a quasiequilibrium distribution representing the state after a sudden reversal of the magnetic field, the short-time behavior will be dominated by clusters that were fairly large at the outset and again Eq. (17) may be trusted. In [25] Van Beijeren gave explicit expressions for the short-time behavior, which may be used if the latter is well approximated by a diffusion equation in an external potential. In the present case these cannot be used, since on the relevant time scales the hopping process between neighboring cluster sizes is not well-approximated by a diffusion process. And since the hopping rates depend on cluster size no exact expressions for the short-time behavior are available. But the numerical solution of the master equation (3) gives a very good agreement with the results from our Monte Carlo simulation of the nucleation process, as was shown in Fig. 5.

Besides the free energy as a function of cluster size our calculations require the transition rates $\Gamma_{C,C\pm1}$ between neighboring values of the cluster size. These we estimated by setting them proportional to the mean circumference of a cluster, determining the proportionality constant from the simulated mobility of a straight interface in cylindrical geometry and imposing the detailed balance condition (4).

In our estimations we have been using a number of assumptions, whose validity is not guaranteed under all conditions.

Strong fields should modify the diffusion coefficient; this effect is neglected. The freedom to modify the field strength within the metastable region is limited though, and long nucleation times, as seen mostly in real experiments, require weak fields.

The diffusion coefficient is assumed to be determined by the size of the cluster alone, and is calculated on the assumption that its shape is strictly spherical. This requires that the temperature is not too low, because at very low temperatures the equilibrium shape of the cluster is more square than circular [23]. (This however, is an effect that may easily be corrected for without making any basic changes in the theory.) On the other hand the temperature should not be too close to the critical temperature for shape fluctuations to be reasonably small. To some extent these fluctuations are taken into account, since our calculation of the diffusion coefficient is done for a fluctuating interface around a cylinder. But it is by no means certain that the fluctuations of a circular interface are in all aspects comparable to those of the interface around the cylinder.

It may happen that a cluster splits up or that two clusters merge, corresponding in our theoretical framework to nonzero transition rates $\Gamma_{C,C+i}$ and $\Gamma_{C+i,C}$ with $i > 1$. This effect also is partly accounted for through the numerical determination of the diffusion constant on a cylinder, but especially for larger clusters the difference in geometry may cause additional effects. However, these will only become important in systems that contain a sizable density of clusters of spins aligned with the external field. Hence, also this approximation can be trusted least near the critical point.

No memory effects are accounted for explicitly. For spin-flip dynamics, memory effects will chiefly be due to the influence of shape fluctuations on the transition rates. Since shape fluctuations on larger length scales will decay only slowly, these may be fairly long-lasting effects. Again, our way of determining the diffusion coefficient will take many of these effects into account implicitly, but memory effects involving large shape fluctuations may be different for the present cluster geometry. For magnetization conserving dynamics (consisting, e.g., of local spin exchanges) much stronger memory effects exist due, e.g., to the effect that a spin that is released from a large cluster has high probability of reattaching to it soon.

Under conditions in which the effects above are negligible, our theoretical framework is capable of estimating nucleation rates with an accuracy in the range of 20%. The small systematic overestimation by about 10% of the nucleation time by theory may have several causes. The radius of a cluster will be slightly larger than our estimate because especially a large cluster will typically contain a few holes in its interior. Since the equilibrium magnetization is always larger than 0.92 for the temperatures studied, the density of vacancies in the cluster is less than 4%, and hence the increase in interface length due to holes is less than 2%. Also the assumptions that the diffusion coefficient is independent of the magnetic field and of the orientation of the interface may be not entirely correct. At low temperatures a diagonal interface is much more mobile than a straight one, but at the fairly elevated temperatures studied here one would not expect a large orientation dependence. Further there could be effects from the possibility of cluster splittings and mergings, though some of these are accounted for through our numerical determination of the diffusion constant on a cylinder.

We are currently extending our investigations to two-dimensional Ising systems with magnetization-conserving dynamics as well as to three-dimensional Ising systems.

APPENDIX

To illustrate the dependence of the interface diffusion coefficient on the system size and on the type of boundary conditions, as discussed in Sec. IV B, we consider diffusion in a two-dimensional BCSOS model with stochastic dynamics. This model is much simpler than the Ising model and

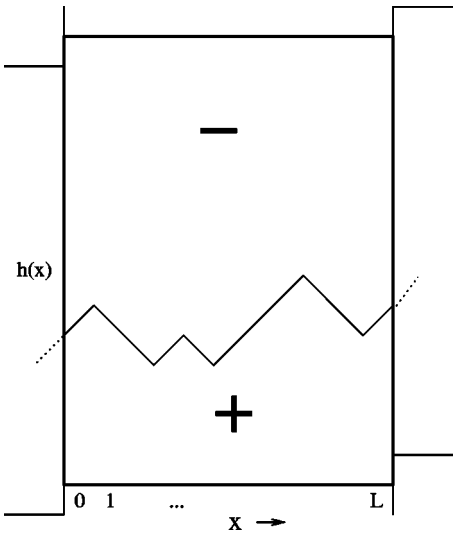

FIG. 6. Example of an interface configuration in the two-dimensional BCSOS model, with horizontally helical and vertically antiperiodic boundary conditions.

allows for an explicit determination of the diffusion constant as a function of system size and helicity conditions. It is illustrated in Fig. 6.

An interface consists of a sequence of straight segments with unit length, oriented with an angle of $+45°$ (or "up") or $-45°$ (or "down") with respect to the horizontal axis; it separates a completely filled crystal phase from a completely empty vacuum. The interface dynamics consists of evaporation of crystal sites at "peak sites" (consecutive segments oriented up and down) and the deposition of such units at "valley sites" (consecutive segments oriented down and up). When the rates of evaporation and of deposition are equal, the interface performs normal diffusion in the vertical direction, corresponding to a diffusive time evolution of the total mass below the interface. The diffusion constant for this process is easily seen to be equal to the average number of peaks (equal to the number of valleys) in the interface. The determination of this number in equilibrium is a simple combinatorial problem. However, one should treat the boundary conditions properly. In the case of periodic boundary conditions in the horizontal direction, the total numbers of segments up and down have to be equal. Helical boundary conditions may be imposed by requiring m segments up and n segments down, with $m \neq n$; we will call these boundary conditions (m,n). The equilibrium distribution assigns equal weights to all configurations with the proper values of m and n; one easily sees that this satisfies the detailed balance conditions for the chosen jump rates. The diffusion coefficient may now be expressed as

$$D(m,n) = \Gamma n_g(n,m), \tag{A1}$$

with Γ the rate of evaporation and deposition, and $n_g(n,m)$ the average number of peak sites or valley sites in the system. For $n_g(n,m)$ a simple recursion relation is obtained through the following reasoning: all configurations with boundary conditions (m,n) may be constructed from all configurations with $(m,n-1)$ by adding a down segment at the position just following one of the m up segments. (In fact each new configuration is obtained precisely m times this way, but that does not change the reasoning.) If the segment is added at the end of a cluster of up segments it does not increase the number of peaks. On average there are $n_g(n-1,m)$ positions where this will happen. In all other cases the number of peaks is increased by one. As a result one obtains the recursion relation

$$n_g(n,m) = n_g(n-1,m) + 1 - \frac{n_g(n-1,m)}{m}$$

$$= 1 + \frac{m-1}{m} n_g(n-1,m). \tag{A2}$$

One easily finds that this recursion relation is solved by

$$n_g(n,m) = m\left[1 - \left(\frac{m-1}{m}\right)^n\right]. \tag{A3}$$

When m is large this yields

$$n_g(n,m) = m\left(1 - \frac{1}{e}\right) + \frac{1}{2e},$$

for periodic boundary conditions $(n=m)$, and

$$n_g(n,m) = m\left(1 - \frac{1}{e}\right) - \frac{1}{2e}$$

for helical boundary conditions with $n=m\pm1$. For the Ising model these results can be applied directly to the case of sloped boundaries at very low temperatures, but for higher temperatures calculations would become much harder. Our main point here is to show that generically a constant term is to be expected in Eq. (21), in addition to a linear one.

[1] P. G. Debenedetti, *Metastable Liquids* (Princeton University Press, Princeton, NJ, 1996).
[2] P. A. Rikvold and B. M. Gorman, in *Annual Reviews of Computational Physics I*, edited by D. Stauffer (World Scientific, Singapore, 1994), pp. 149–191.
[3] M. Volmer and A. Weber, Z. Phys. Chem., Stoechiom. Verwandtschaftsl. **119**, 277 (1926).
[4] Z. Farkas, Z. Phys. Chem., Stoechiom. Verwandtschaftsl. **125**, 236 (1927).
[5] R. Becker and W. Döring, Ann. Phys. **24**, 719 (1935).
[6] J. B. Zeldovich, Acta Physicochim. URSS **18**, 1 (1943).
[7] P. A. Rikvold, H. Tomita, S. Miyashita, and S. W. Sides, Phys. Rev. E **49**, 5080 (1994).
[8] M. A. Novotny, P. A. Rikvold, M. Kolesik, D. M. Townsley, and R. A. Ramos, J. Non-Cryst. Solids **274**, 356 (2000).
[9] V. A. Shneidman, K. A. Jackson, and K. M. Beatty, Phys. Rev.

B **59**, 3579 (1999).
[10] S. Auer and D. Frenkel, Nature (London) **409**, 1020 (2001).
[11] J. L. Harland and W. van Megen, Phys. Rev. E **55**, 3054 (1997).
[12] L. Gránásy and T. Pusztai, J. Chem. Phys. **117**, 10121 (2003).
[13] M. Acharyya and D. Stauffer, Eur. Phys. J. B **5**, 571 (1998).
[14] V. A. Shneidman, K. A. Jackson, and K. M. Beatty, J. Chem. Phys. **111**, 6932 (1999).
[15] Th. Neuhaus and J. S. Hager, J. Stat. Phys. **113**, 47 (2003).
[16] N. Metropolis, A. W. Rosenbluth, M. N. Rosenbluth, A. H. Teller, and E. Teller, J. Chem. Phys. **21**, 1087 (1953).
[17] K. Brendel, G. T. Barkema, and H. van Beijeren, Phys. Rev. E **67**, 026119 (2003).
[18] A. Coniglio and W. Klein, J. Phys. A **12**, 2775 (1980).
[19] P. Hänggi, P. Talkner, and M. Borkovec, Rev. Mod. Phys. **62**, 251 (1990).
[20] M. E. J. Newman and G. T. Barkema, *Monte Carlo Methods in Statistical Physics* (Oxford University Press, Oxford, 1999).
[21] R. C. Tolman, J. Chem. Phys. **17**, 333 (1949).
[22] L. Onsager, Phys. Rev. **65**, 117 (1944).
[23] J. E. Avron, H. van Beijeren, L. S. Schulman, and R. K. P. Zia, J. Phys. A **15**, L81 (1982).
[24] K. Brendel, G. T. Barkema, and H. van Beijeren (unpublished).
[25] H. van Beijeren, J. Stat. Phys. **110**, 1397 (2003).